TECHNICAL NOTE

Special Section: Tribute to Rien van Genuchten, Recipient of the 2023 Wolf Prize for Agriculture

Implementation of the Brunswick model system into the Hydrus software suite

Efstathios Diamantopoulos[1] | **Jirka Simunek[2]** | **Tobias K. D. Weber[3]**

[1]Chair of Soil Physics, University of Bayreuth, Bayreuth, Germany

[2]Department of Environmental Sciences, University of California, Riverside, California, USA

[3]Soil Science Section, University of Kassel, Witzenhausen, Germany

Correspondence
Efstathios Diamantopoulos, University of Bayreuth, Bayreuth, Germany. Email:
efstathios.diamantopoulos@uni-bayreuth.de

Abstract

The Brunswick modular framework for modeling unsaturated soil hydraulic properties (SHP) over the full moisture range was implemented in the Hydrus suite. Users can now additionally choose between four different variants of the Brunswick model: (i) van Genuchten–Mualem (VGM), (ii) Brooks–Corey, (iii) Kosugi, and (iv) modified van Genuchten. For demonstration purposes, simulation results for two different setups, (i) bare soil evaporation and (ii) root water uptake, are presented, along with a comparison of the original VGM model and its Brunswick variant. Results show that the original VGM model underestimates the simulated cumulative evaporation and cumulative transpiration due to the inconsistent representation of the SHP in the dry moisture range. We also implemented a two-step hydro-PTF (pedotransfer function) into the Hydrus suite that converts the parameters of the original VGM model (from Rosetta) to the corresponding Brunswick variant. In that way, physically comprehensive simulations are ensured if no data on SHP are directly available, but information on physical soil properties (e.g., texture and bulk density) exists.

1 | INTRODUCTION

Accurate simulations of water dynamics in soils with the Richards–Richardson equation (Richards, 1931; Richardson, 1922) require the correct representation of the soil hydraulic properties (SHP) from saturation to very dry conditions (Iden et al., 2021). According to Weber et al. (2023), we can easily obtain 200 different models of SHPs if we combine the 22 water retention models listed in Du et al. (2016) with the 9 models of relative conductivity presented by Assouline and Or (2013). Among all those models, the most widely used model for representing SHP is by far the van Genuchten–Mualem

model (VGM) (Mualem, 1976; van Genuchten, 1980). During the last years, many different models have been proposed in the literature with the aim to extend or replace the VGM model, with the focus either on the wet range or the dry range (Fayer & Simmons, 1995; Lebeau & Konrad, 2010; Peters, 2013; Vogel et al., 2000), among hundreds of others. Such a system for modeling SHPs was presented by Weber et al. (2019), which, for the most popular model configuration, comes with a pedotransfer function to predict the model parameters (Weber et al., 2020).

In this technical note, we present implementations of the Brunswick model variants (Streck & Weber, 2020) into the Hydrus suite, Version 5. These models are: (i) van Genuchten-Mualem (VGM) (Mualem, 1976; van Genuchten, 1980), (ii) Brooks–Corey (BC) (Brooks & Corey, 1964), (iii) Kosugi (KS) (Kosugi, 1996a), and (iv) modified van Genuchten (modVGM) (Vogel & Cislerova, 1988). As an example, we

---

Abbreviations: BC, Brooks-Corey; BW, Brunswick; Cum. Transp., cumulative transpiration; PTF, pedotransfer function; KS, Kosugi; modVGM, modified van Genuchten; RWU, root water uptake; SHP, soil hydraulic properties; VGM, van Genuchten-Mualem.

compared the performance of the classical VGM model to the Brunswick variant (VGM-BW). For this, we first fitted the two models to water retention and unsaturated hydraulic conductivity data for three soils with contrasting properties. Second, for the three selected soil types, we tested the difference between the two SHPs models by conducting two different simulations: (i) bare soil evaporation and (ii) root water uptake (RWU). For the RWU simulations, we used two different models: the Feddes model (Feddes et al., 1978) and the Nimah–Hanks model (Nimah & Hanks, 1973). The main difference between the two models is that in the Nimah–Hanks model RWU is calculated using the unsaturated hydraulic conductivity of the local soil and the pressure head gradient between the soil and the roots, whereas, in the Feddes model, the local pressure head determines actual uptake. Third, we discuss the systematic differences in the simulation results, identifying the relevance of including a comprehensive representation of the SHP in the dry range. Finally, we present the equations for all BW variants implemented in Hydrus in the Appendix.

2 | MATERIAL AND METHODS

In the following paragraphs, we present the governing equation of water flow in soils, the different models for SHP, and the simulation setups in Hydrus.

2.1 | Water flow in soils

Water fluxes in unsaturated isotropic soils are described by the RE (Richards, 1931; Richardson, 1922) assuming RWU is represented as a sink term:

$$\frac{\partial \theta(h)}{\partial t} = -\nabla \cdot \mathbf{q} - \Gamma_{\text{roots}} = \nabla \cdot [K(h)\nabla h] + \frac{\partial K(h)}{\partial z} - \Gamma_{\text{roots}}, \tag{1}$$

where z is the vertical coordinate [L], h is the pressure head [L], θ is the volumetric water content [L^3 L^{-3}], $\mathbf{q}$ is the Darcy flux [L T^{-1}], K [L T^{-1}] is the saturated/unsaturated hydraulic conductivity as a function of θ or h, and Γ_{roots} is the sink term representing RWU [T^{-1}]. Equation (1) requires that the air pressure in the soil is equal to the atmospheric pressure (single-phase flow) and that a local equilibrium between water content and pressure head is always valid (Diamantopoulos & Durner, 2012) and is described by the water retention curve $\theta(h)$.

2.2 | Models for SHPs

In the following, we limit the description of the SHP to a minimum. The full mathematical expressions for all original and extended models are provided in Appendix A.1–A.4.

> **Core Ideas**
>
> - A modular framework was implemented in Hydrus to describe soil hydraulic properties.
> - The new model is more robust in describing soil hydraulic properties in the dry moisture range.
> - Hydrus simulations with the new model predict high bare soil evaporation and transpiration fluxes.

2.2.1 | The classical approach

In the classical approaches, the water retention curve is described as a function of the pressure head:

$$\theta(h) = \theta_r + (\theta_s - \theta_r)\Phi_e(h), \tag{2}$$

where $\Phi_e(h)$ is the effective water saturation function, with values between 1.0 and 0.0, and θ_s [L^3 L^{-3}] and θ_r [L^3 L^{-3}] are the saturated and residual water contents, respectively.

The unsaturated hydraulic conductivity is given as a function of the pressure head by:

$$K(h) = K_s K_r(h), \tag{3}$$

where K_r [-] is the relative unsaturated hydraulic conductivity function, which is scaled with the saturated hydraulic conductivity, K_s [L T^{-1}]. Full expressions for $\Phi_e(h)$ and $K_r(h)$ are given in Appendix A.2–A.5 for all four models presented in the introduction.

2.2.2 | The VGM-BW model

According to Weber et al. (2019), the SHP in Equations (2) and (3) may be extended using the Brunswick model framework. Therein, the soil water retention and the unsaturated hydraulic conductivity are partitioned into two domains. One represents water stored and conducted in completely filled capillaries, and another one water stored and conducted in partially full pores. These two domains are, respectively, named the *capillary* (suffix c) and the *non-capillary* (suffix nc) pore domains. The water retention function in BW is given as:

$$\theta(h) = \theta_{sc} S_c(h) + \theta_{snc} S_{nc}(h), \tag{4}$$

where θ_{sc} [L^3 L^{-3}] and θ_{snc} [L^3 L^{-3}] are the saturated water content values of the respective domains. $S_c(h)$ [-] and $S_{nc}(h)$ [-] describe the effective water saturation as a function of the pressured head, respectively. The function $S_c(h)$ is a rescaled

$\Phi_e(h)$ by

$$S_c(h) = \frac{\Phi_e(h) - \Phi_e(h_0)}{1 - \Phi_e(h_0)}. \tag{5}$$

This ensures a water content of 0 at a fixed very low pressure head, here $h_0 = -10^{6.8}$ cm, as it is described in Appendix A.1.

The unsaturated hydraulic conductivity function is given by

$$K(h) = K_{sc}K_{rc} + K_{snc}K_{rnc}. \tag{6}$$

Again, c and nc stand for the capillary and non-capillary pore domains, K_{sc} [L T^{-1}] and K_{rc} [-] are the saturated and relative hydraulic conductivities of the capillary pore domain, and likewise, K_{snc} [L T^{-1}] and K_{rnc} [-] the saturated and relative hydraulic conductivities of the non-capillary pore domain. Note that the full BW model framework includes a term for isothermal vapor conductivity. In Hydrus, the option to simulate isothermal vapor conductivity is a standard feature that can be selected and, therefore, not included here.

2.3 | Modeling soil evaporation

In Hydrus, evaporation dynamics at the soil surface are simulated by assuming a Neumann-type boundary condition. The water flux at the soil surface, q_{top} [L T^{-1}], is set equal to the potential evaporation flux ($q_{Pot. E.}$) [L T^{-1}], provided by the user. However, if the $h_{soil}(z = 0)$ [L] becomes equal or less than a critical pressure head h_{crit} [L], the boundary condition is switched to a Dirichlet-type boundary condition with $h_{soil}(z = 0) = h_{crit}$ [L]. In that way, the potential evaporation rate is reduced to the actual evaporation rate, and it is calculated by applying the Darcy law to the soil surface. For more information, we refer to Šimunek et al. (2006).

2.4 | Modeling RWU

We calculated Γ_{roots} in Equation (1) based on the two macroscopic approaches of Feddes et al. (1978) and Nimah and Hanks (1973). In this technical note, we do not present the models systematically but focus on the basic differences between them. For full details about the two models, we refer to the original publications of Feddes et al. (1978) and Nimah and Hanks (1973), respectively. The model of Feddes et al. (1978) calculates Γ_{roots}, based on potential transpiration and on the soil pressure head $h_{soil(z)}$ at each numerical node, by applying a stress function $\alpha(h)$, which varies between 0 and 1 (1: no water stress, 0: no RWU). In the model of Nimah and Hanks (1973), Γ_{roots} is calculated by the difference between the "effective" pressure head at the root surface, $h_{root}(z)$ and $h_{soil}(z)$, and the unsaturated hydraulic conductivity of the soil

at each depth, calculated from Equations (3) and (6) for the two SHP models, respectively. The main difference between the two models is that for the same values of $h_{soil}(z)$ and for the same plant (the same stress function, $\alpha(h)$), the model of Feddes et al. (1978) will calculate the same Γ_{roots} for any soil. This is different in the model of Nimah and Hanks (1973), in which the conductivity curve controls the RWU calculations.

2.5 | Experimental data

We fitted the VGM and VGM-BW models to experimental water retention and conductivity data for three different soils from the recently published database of Hohenbrink et al. (2023). We selected a very sandy soil (Sand) (99.8%, sampleID: "KIT_063"), a clay loam soil (CLoam) (37.4% sand, 34.1% loam, and 28.5% clay, sampleID: "TUBS_106"), and a clay soil (Clay) (66.4% clay, sampleID: "KIT_140"). Details about the experimental protocol can be found in Hohenbrink et al. (2023). We followed the fitting protocol for tabulated SHPs data as in Diamantopoulos and Durner (2015) and Peters and Durner (2008). The parameters for the three soils and two models are presented in Tables 1 and 2.

2.6 | Simulation setup

2.6.1 | Evaporation

We assumed a 10-cm-long soil profile with a uniform initial pressure head distribution, a zero flux at the bottom of the column, and a potential evaporation rate of 0.5 cm day^{-1} at $z = 0$ cm. In total, we ran six simulations for three different soil types, parameterized with the VGM and VGM-BW models.

2.6.2 | Root water uptake

We assumed a 150-cm long soil profile with a uniform initial pressure head distribution. We assumed a seepage face boundary condition at the bottom of the profile and a linearly decreasing RWU distribution with depth. Similarly, as for evaporation experiments, we ran simulations for three different soils and two RWU models. Finally, we assumed the potential transpiration rate equal to 0.5 cm day^{-1}. The critical pressure heads for the Feddes model were set to: $P0 = -10$ cm, $POpt = -25$ cm, $P2H = -320$ cm, $P2L = -600$ cm, and $P3 = -16,000$ cm (Sugar Beet; Wesseling et al., 1991). For the Nimah and Hanks model, the maximum value of the pressure head that the roots can apply was assumed to be equal to -16,000 cm or pF = 4.2 (wilting point).

TABLE 1 Parameters for the van Genuchten–Muealem model for three different soils.

Soil type	θ_r [-]	θ_s [-]	α [cm^{-1}]	n [-]	K_s [cm day^{-1}]	λ [-]
Sand	0.059	0.306	0.0213	3.4	74.9	−0.4
CLoam	0.217	0.679	0.149	1.1	1000	−0.5
Clay	0.059	0.608	0.015	1.1	8.6	4.6

TABLE 2 Parameters for the van Genuchten–Muealem model to the Brunswick variant model for three different soils. For all the simulations with this model, we fixed $a = 1.5$ and $h_0 = 10^{6.8}$.

Soil type	θ_{snc} [-]	θ_{sc} [-]	α [cm^{-1}]	n [-]	K_{sc} [cm day^{-1}]	K_{snc} [cm day^{-1}]	λ [-]
Sand	0.063	0.242	0.021	3.5	74.3	0.0	−0.4
CLoam	0.400	0.257	0.111	2.8	71.0	0.17	−1.7
Clay	0.000	0.611	0.020	1.1	80.0	1e-3	10.0

2.7 | Initial conditions

As the primary emphasis of this study lies in the representation of the dry range of SHPs, we deliberately selected distinct initial pressure heads for the three soil types (green lines in Figure 1). This ensures that any variations in the simulation results arise exclusively from the representation of the dry range in the two models and not from the wet range.

3 | RESULTS AND DISCUSSION

3.1 | Fitting of VGM and VGM-BW to data

Both the VGM and VGM-BW models describe the water retention and conductivity data in the wet range very well (Figure 1, Tables 1 and 2). Any disparities visible in the wet range between the two models can be attributed to the absence of conductivity data in the wet range, along with compensation made by the fitting algorithm to characterize data in the dry range (mostly retention data), accounting for limitations inherent in the models, especially in the VGM model. However, the difference between the VGM and VGM-BW models becomes apparent in describing the dry range of both curves, since the VGM model predicts an almost constant and non-zero water content for pF >2.5 (h in cm) for the Sand, pF > 4 for the CLoam, and pF > 6.8 for the Clay, respectively. On the other hand, the VGM-BW model describes the retention data in the dry range very well, showing an almost linear decrease of the water content versus pF in that range, guaranteeing by definition that water content will be zero around a value of pF = 6.8 (in cm) ("oven dryness," (Blöcher et al., 2023)). It has also been shown before that this dry component in the water retention curves is required for simulating bare soil evaporation at the continuum scale (Iden et al., 2021, 2021; Saito

et al., 2006). For the conductivity data, both models perform almost equally, with a distinct change in the slope around pF = 2.5 for the Sand, which is typical for corner and/film flow (Diamantopoulos & Durner, 2015; Tuller & Or, 2001) components. Only the VGM-BW model can describe this change in slope in the logK versus pF data, while the VGM model cannot (Figure 1).

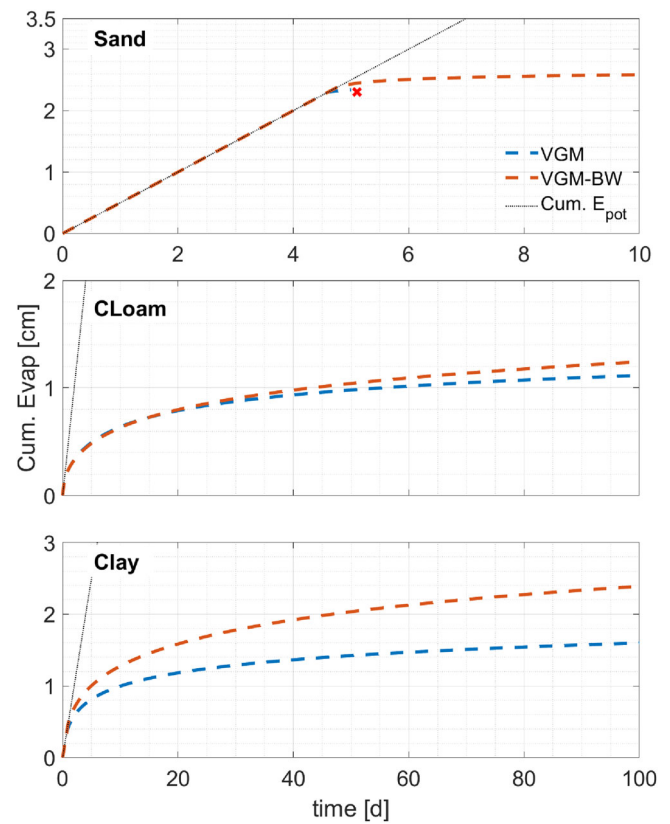### 3.2 | Simulations of bare soil evaporation

For all three soils, the simulations with the VGM-BW model yielded a higher Cumulative Evaporation value (Cum. Evap.) at the end of the simulation (Figure 2). The difference was low (around 0.2 cm) for the Sand and CLoam soil and slightly higher for the Clay soil (around 0.8 cm). For the VGM model, the simulation for the Sand did not finish because Hydrus experienced numerical problems due to the constant water content value after pF > 2.5 (Figure 2, top, red x sign). Although the differences in Cum. Evap. were low, more important implications is that for the Sand and CLoam soil, the simulations predict a later time for stage 2 evaporation to be reached when the water content at the top of the soil equals 0.069 cm^3 cm^{-3} and 0.217 cm^3 cm^{-3}, respectively. This is physically implausible since, under prolonged high atmospheric demand, we expect a near zero water content at the top of the soil surface, with corresponding effects on the water content profiles. We note that Iden et al. (2021) have illustrated that a correct description of bare soil evaporation experiments of different soils with isothermal Richards equation requires a water retention model that ensures a zero water content at oven dryness (Saito et al., 2006), as well as a film component in the conductivity function, and an isothermal vapor conductivity component which is not included in our simulations.
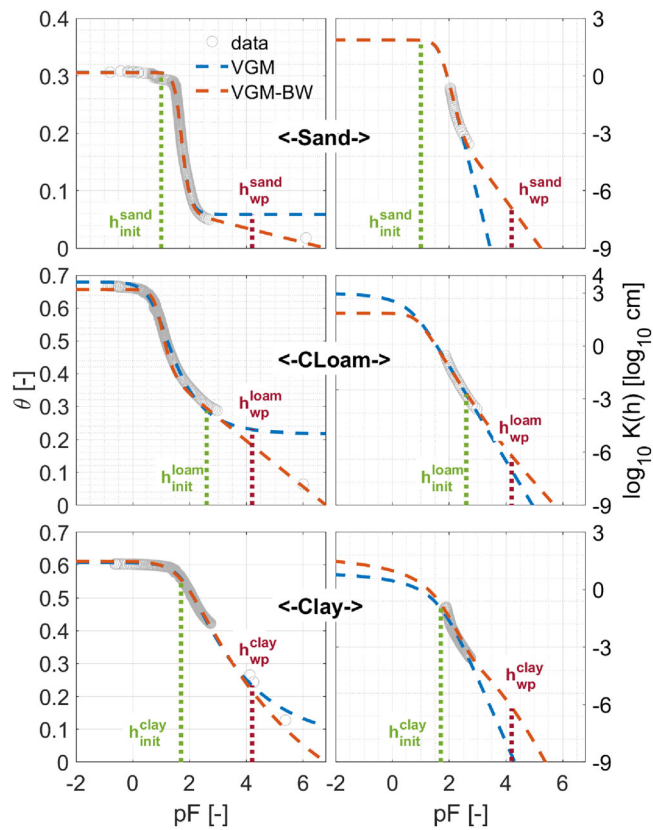
FIGURE 1 Water retention curves (left column) and hydraulic conductivity curves right column) for the three soils and for the van Genuchten–Mualem model (VGM) and VGM model to the Brunswick variant models. The green line shows the initial value of the pressure head for each soil type and for all simulations. The red line shows the pressure head at the wilting (-16,000 cm or pF=4.2) point for both RWU models.

FIGURE 2 Cumulative actual evaporation for the three soil types (rows) and the two soil hydraulic property models (blue line: van Genuchten-Mualem model [VGM], orange line: VGM model to the Brunswick variant). For the VGM model and for the Sandy soil, the simulation could not be completed because once the soil reaches the residual water content, no water can be removed by evaporation and numerical problems occur (red X sign in the top figure).
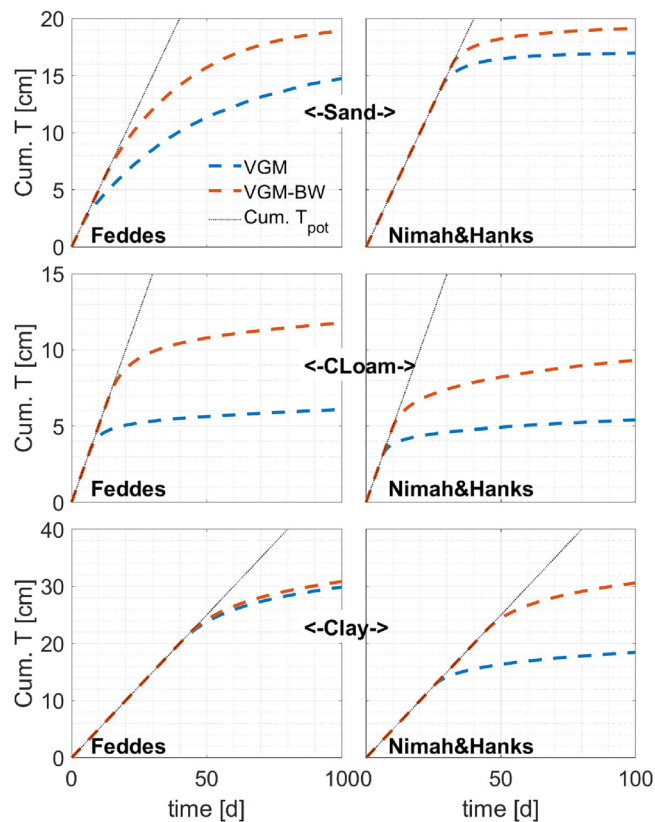
3.3 | Simulations of root water uptake

For all three soils and the two RWU models, the simulations with the VGM-BW model yielded a higher Cumulative Transpiration value (Cum. Transp.) at the end of the simulation (Figure 3, left panel). For the Feddes model, the difference in the final value of Cum. Transp. for the Sand and CLoam soils was around 4 and 6 cm, respectively. This is due to the shape of the water retention curve in the dry range: from the wet range until the permanent wilting point (in our simulation $h_{wp} = -16,000$ cm or $pF_{wp} = 4.2$) and the concept of residual water content. For the VGM model, the retention curve shows a change in slope at around the residual water content, indicating less water capacity for RWU. This is especially visible for the Sandy and CLoam soils. Due to this change in slope in the dry range, the VGM simulation reaches the wilting point pressure head faster than the VGM-BW model and, therefore, transpiration stops. This is not the case for the VGM-BW model due to the linear part of the water retention curve (Figure 1) in the dry range. For VGM-BW, deviation

from the cumulative potential transpiration line (black line in Figure 3) always starts later than for VGM. This difference is very small for the Clay soil since, until $pF_{wp} = 4.2$, both retention curves are similar (Figure 1, bottom left).

Similar to the Feddes model, the VGM-BW model yielded higher values of Cum. Transp. at 100 days (Figure 3, right panel) for the Nimah and Hanks RWU model. For the Sand, both the VGM and VGM-BW simulations show a longer period where actual transpiration is equal to potential, which indicates an inherent compensation built in the model of Nimah and Hanks, where the roots can apply higher suction to satisfy the demand. However, after a critical time (different for the two SHP models), actual transpiration is reduced due to the lower conductivity of the dryer soil. We note that at the end of the simulation, the VGM model simulates a pressure head of –3100 cm, residual water content, and very low conductivity on the order of 10^{-9} cm day^{-1} at the soil surface (dryer node due to higher root length density). On the contrary, for the VGM-BW model, these values were -11,000 cm, 0.04 cm^3 cm^{-3}, and 10^{-6} cm day^{-1}, respectively. For the CLoam soil,

FIGURE 3 Cumulative actual transpiration for the three soil types (rows), the two root water uptake models (left: Feddes, right: Nimah & Hanks), and the two soil hydraulic property models (blue line: van Genuchten-Mualem model [VGM], orange line: VGM model to the Brunswick variant).

due to the lower h_{init}, the drop in the hydraulic conductivity is the limiting factor for reducing actual transpiration and overall lower uptake values in comparison with the Feddes model. For the clay soil, differences between VGM and VGM-BW are larger due to the larger differences in the unsaturated conductivity for the two models (Figure 1, right panel). We note that the change of the slope in the conductivity data in the dry range can be a result of corner flow (Diamantopoulos & Durner, 2015) and/or film flow (Tuller & Or, 2001). Convincing experimental evidence of this change in slope exists for sandy soils, but not for heavier soil classes, meaning that our results, especially for the CLoam and Clay soil and the Nimah and Hanks model, should be interpreted with caution, since no change in the slope in the conductivity data can be observed or hypothesized.

Overall, there are significant differences between the simulation results with the VGM and VGM-BW models concerning bare soil evaporation and RWU with the Hydrus suite. This indicates the high need for water retention and unsaturated conductivity data of high quality, especially in the dry range, and SHP models that can describe those data accurately (Peters, 2013; Weber et al., 2019). This can now be done in Hydrus by the use of the Brunswick model as well as

with the use of a two-step hydro-PTF functions (Weber et al., 2020), that allow the conversion of the VGM parameters to the VGM-BW parameters. This guarantees more physically coherent simulations if SHP data are missing.

4 | CONCLUSIONS

We implemented the Brunswick modular SHP model and the two-step hydro-pedotransfer function of Weber et al. (2020) in the Hydrus suite. The model allows for a more physically coherent representation of the water retention and hydraulic conductivity curves in the dry range. We also show that the widely used VGM model may underestimate bare soil evaporation and transpiration when compared to the Brunswick model. Given the simulation results of this study, we suggest replacing the VGM model with the VGM-BW model, especially for simulations under arid conditions. Future work will target the implementation of the bimodal version of the VGM-BW model into the Hydrus suite.

AUTHOR CONTRIBUTIONS

Efstathios Diamantopoulos: Conceptualization; data curation; formal analysis; investigation; methodology; software; visualization; writing—original draft; editing. **Jirka Simunek**: Software; writing—original draft; editing. **Tobias K. D. Weber**: Writing—original draft; editing.

ORCID

Efstathios Diamantopoulos https://orcid.org/0000-0001-7870-0291
Jirka Simunek https://orcid.org/0000-0002-0166-6563
Tobias K. D. Weber https://orcid.org/0000-0002-3448-5208

REFERENCES

Assouline, S., & Or, D. (2013). Conceptual and parametric representation of soil hydraulic properties: A review. *Vadose Zone Journal*, *12*(4), 1–20. https://doi.org/10.2136/vzj2013.07.0121

Blöcher, J. R., Diamantopoulos, E., Durner, W., & Iden, S. C. (2023). Validating coupled flow theory for bare-soil evaporation under different boundary conditions. *Vadose Zone Journal*, *22*(6), e20277. https://doi.org/10.1002/vzj2.20277

Brooks, R. H., & Corey, A. T. (1964). *Hydraulic properties of porous media* (Hydrology Papers No 3). Colorado State University.

Diamantopoulos, E., & Durner, W. (2012). Dynamic nonequilibrium of water flow in porous media: A review. *Vadose Zone Journal*, *11*(3), 0197. https://doi.org/10.2136/vzj2011.0197

Diamantopoulos, E., & Durner, W. (2015). Closed-form model for hydraulic properties based on angular pores with lognormal size distribution. *Vadose Zone Journal*, *14*(2), 1–7. https://doi.org/10.2136/vzj2014.07.0096

Du, E., Di Vittorio, A., & Collins, W. D. (2016). Evaluation of hydrologic components of community land model 4 and bias identification. *International Journal of Applied Earth Observation and Geoinformation*, *48*, 5–16.

Fayer, M. J., & Simmons, C. S. (1995). Modified soil water retention functions for all matric suctions. *Water Resources Research*, *31*(5), 1233–1238.

Feddes, R. A., Kowalik, P. J., & Zaradny, H. (1978). Water Uptake by plants. In *Simulation of field water use and crop yield* (pp. 16–30). Wiley.

Hohenbrink, T. L., Jackisch, C., Durner, W., Germer, K., Iden, S. C., Kreiselmeier, J., Leuther, F., Metzger, J. C., Naseri, M., & Peters, A. (2023). Soil water retention and hydraulic conductivity measured in a wide saturation range. *Earth System Science Data Discussions*, *2023*, 1–20.

Iden, S. C., Blöcher, J. R., Diamantopoulos, E., & Durner, W. (2021). Capillary, film, and vapor flow in transient bare soil evaporation (1): Identifiability analysis of hydraulic conductivity in the medium to dry moisture range. *Water Resources Research*, *57*(5), e2020WR028513.

Iden, S. C., Diamantopoulos, E., & Durner, W. (2021). Capillary, film, and vapor flow in transient bare soil evaporation (2): Experimental identification of hydraulic conductivity in the medium to dry moisture range. *Water Resources Research*, *57*(5), e2020WR028514.

Kosugi, K. (1996). Lognormal distribution model for unsaturated soil hydraulic properties. *Water Resources Research*, *32*(9), 2697–2703.

Lebeau, M., & Konrad, J.-M. (2010). A new capillary and thin film flow model for predicting the hydraulic conductivity of unsaturated porous media. *Water Resources Research*, *46*(12), W12554.

Mualem, Y. (1976). A new model for predicting the hydraulic conductivity of unsaturated porous media. *Water Resources Research*, *12*(3), 513–522.

Nimah, M., & Hanks, R. (1973). Model for estimating soil water, plant, and atmospheric interrelations: II. Field test of model. *Soil Science Society of America Journal*, *37*(4), 528–532. https://doi.org/10.2136/sssaj1973.03615995003700040019x

Peters, A. (2013). Simple consistent models for water retention and hydraulic conductivity in the complete moisture range. *Water Resources Research*, *49*(10), 6765–6780.

Peters, A., & Durner, W. (2008). Simplified evaporation method for determining soil hydraulic properties. *Journal of Hydrology*, *356*(1-2), 147–162.

Richards, L. A. (1931). Capillary conduction of liquids through porous mediums. *Journal of Applied Physics*, *1*(5), 318–333.

Richardson, L. F. (1922). *Weather prediction by numerical process*. Cambridge University Press.

Saito, H., Šimůnek, J., & Mohanty, B. P. (2006). Numerical analysis of coupled water, vapor, and heat transport in the vadose zone. *Vadose Zone Journal*, *5*(2), 784–800. https://doi.org/10.2136/vzj2006.0007

Šimůnek, J. (2006). *Models of water flow and solute transport in the unsaturated zone*, Encyclop. American Cancer Society.

Šimůnek, J., Van Genuchten, M. Th., & Šejna, M. (2006). *The HYDRUS software package for simulating two-and three-dimensional movement of water, heat, and multiple solutes in variably-saturated media* (Technical Manual Version 1.0). PC Progress.

Streck, T., & Weber, T. K. D. (2020). Analytical expressions for non-capillary soil water retention based on popular capillary retention models. *Vadose Zone Journal*, *19*(1), e20042. https://doi.org/10.1002/vzj2.20042

Tokunaga, T. K. (2009). Hydraulic properties of adsorbed water films in unsaturated porous media. *Water Resources Research*, *45*(6), 460.

Tuller, M., & Or, D. (2001). Hydraulic conductivity of variably saturated porous media: Film and corner flow in angular pore space. *Water Resources Research*, *37*(5), 1257–1276.

van Genuchten, M. Th. (1980). Closed-form equation for predicting the hydraulic conductivity of unsaturated soils. *Soil Science Society of America Journal*, *44*(5), 892–898. https://doi.org/10.2136/sssaj1980.03615995004400050002x

Vogel, T., & Cislerova, M. (1988). On the reliability of unsaturated hydraulic conductivity calculated from the moisture retention curve. *Transport in Porous Media*, *3*, 1–15.

Vogel, T., Gerke, H. H., Zhang, R., & Van Genuchten, M. Th. (2000). Modeling flow and transport in a two-dimensional dual-permeability system with spatially variable hydraulic properties. *Journal of Hydrology*, *238*(1-2), 78–89.

Weber, T. K. D., Durner, W., Streck, T., & Diamantopoulos, E. (2019). A modular framework for modeling unsaturated soil hydraulic properties over the full moisture range. *Water Resources Research*, *55*(6), 4994–5011.

Weber, T. K. D., Finkel, M., Conceição Gonçalves, M., Vereecken, H., & Diamantopoulos, E. (2020). Pedotransfer function for the Brunswick soil hydraulic property model and comparison to the van Genuchten–Mualem model. *Water Resources Research*, *56*(9), e2019WR026820.

Weber, T. K. D., Weihermüller, L., Nemes, A., Bechtold, M., Degré, A., Diamantopoulos, E., Fatichi, S., Filipović, V., Gupta, S., & Hohenbrink, T. L. (2023). Hydro-pedotransfer functions: A roadmap for future development. *Egusphere*. (preprint). https://doi.org/10.5194/egusphere-2023-1860

Wesseling, J., Elbers, J., Kabat, P., & Van Den Broek, B. (1991). Swatre: Instructions for input. internal note, Winand Staring Centre, Wageningen, The Netherlands. *International Waterlogging and Salinity Research Institute, Lahore, Pakistan*.

APPENDIX A: SOIL HYDRAULIC FUNCTIONS AND ANALYTICAL SOLUTIONS

In the following subsections, we first define the non-capillary saturation and conductivity functions, followed by the description of the VGM, BC, and KS models, modified VGM, in the original and BW variants. In each model case, the analytical solutions for the non-capillary saturation model to Equation (A.1) are given. Therefore, we will use the equality $x = \log_{10}(|h|)$ as in the original publication (Streck and Weber, 2020).

A.1 | The BW non-capillary saturation and conductivity functions

To model the non-capillary saturation S_{nc} as a function of pressure head h, (Weber et al., 2019) developed a universal and flexible integral approach. The main advantage is that it can, in principle, be used for any model of $\Phi_e(h)$. In the

following, we adopt the notation by (Streck and Weber, 2020). For convenience, we first introduce $x = \log_{10}(|h|)$. Then we write S_{nc} as a function of x which is given by

$$S_{nc}^{*pF}(x) = \int_{-\infty}^{x} \left(\Phi_e^{pF}(x') - 1 \right) dx' \qquad (A.1)$$

where $\Phi_e^{pF}(x)$ [-] is $\Phi_e(h)$ in $\log_{10}$, and x' is the dummy variable of integration. Streck and Weber (2020) explicitly explain that the integral equals the area between full saturation ($x' = -\infty$, corresponding to $h = 0$ cm) and the capillary saturation at a given pF value. Analytic solutions for special cases of $S_c(h)$ were derived by Streck and Weber (2020). Numerical integration from $-\infty$ is not tractable. Thus, numerical integration is done by replacing $-\infty$ with -3, which corresponds to a pressure head of 10^{-3} cm. Weber et al. (2019) transform Equation (A.1) to normal space by substituting x by h. Using the relationship

$$\frac{dx}{dh} = -\log_{10}(e)\frac{1}{h}, \qquad (A.2)$$

then yields

$$S_{nc}^*(h) = \int_{h}^{-10^\epsilon} \left(\frac{\Phi_e'(h') - 1}{h'} \right) dh'. \qquad (A.3)$$

Since $S_{nc}^*(h)$ neither reaches from 1 at full saturation to 0 at complete dryness, shifting and re-scaling are required, which is achieved by

$$S_{nc}(h) = 1 - \frac{S_{nc}^*(h)}{S_{nc}^*(h_0)} \qquad (A.4)$$

K_{rnc} [-] is a function of the non-capillary saturation (Peters, 2013; Tokunaga, 2009)

$$K_{rnc}(h) = \left(\frac{|h_0|}{h_r} \right)^{-\alpha_s(1-S_{nc}(h)),} \qquad (A.5)$$

where h_r [L] ensures matching dimensions in $K_{rnc}(h)$ and is set to 1 cm. α_s controls the slope of decrease in $K_{rnc}(h)$.

A.2 | The VGM and VGM-BW models
According to van Genuchten (1980), the effective water saturation, Φ_e is given as a function of pressure head by:

$$\Phi_e(h) = [1 + [|\alpha h|]^n]^{-m}, \qquad (A.6)$$

where α [L^{-1}] and n [-] are shape parameters and $m = 1 - 1/n$. The relative unsaturated hydraulic conductivity is given

by:

$$K_r(h) = \Phi_e(h)^\lambda[1 - (1 - \Phi_e^{1/m})^m]^2, \qquad (A.7)$$

where λ [-] is a shape parameter of the conductivity function.

Equations (VGM): 2, 3, A.6, A.7
Parameters (VGM): θ_s, θ_r, α, n, K_s, λ

According to Streck and Weber (2020), the analytical solution of the non-capillary saturation function for the van Genuchten case is given as

$$S_{nc}^{pF}(x) = \frac{1}{n\ln(10)} \left[B(1 + (\alpha 10^x)^n; 1, 0) - B\left(1 + (\alpha 10^x)^n; \frac{1}{n}, 0\right) \right.$$
$$\left. + n - \frac{1}{n} + \left(\frac{1}{n} - 1 \right) \sum_{k=1}^{\infty} \frac{1}{k(k+1)(nk+1)} \right], \qquad (A.8)$$

where B is the incomplete beta function.

The unsaturated hydraulic conductivity of the capillary part (Equation 6) for the VGM variant of the Brunswick model framework is given by

$$K_{rc}(h) = S_c(h)^\lambda \left(1 - \left[\frac{1 - \Phi_e(h)^{1/m}}{1 - \Phi_e(h_0)^{1/m}} \right]^m \right)^2 \qquad (A.9)$$

Equations (VGM-BW): 4, 5, A.6, A.8, 6, A.9, A.5
Parameters (VGM-BW): θ_{sc}, θ_{snc}, α, n, K_{sc}, K_{snc}, λ, α_s, h_0

A.3 | The BC and BC-BW models
The Brooks–Corey (BC) (Brooks & Corey, 1964) effective saturation model is given as a function of pressure head by

$$\Phi_e(h) = \begin{cases} |\alpha h|^{-n} & h < -1/\alpha \\ 1 & h \geq -1/\alpha, \end{cases} \qquad (A.10)$$

with n [-] and α [L^{-1}] as flexible parameters.

The unsaturated hydraulic conductivity function is given by

$$K_r(h) = \Phi_e(h)^{2/n+\lambda+2}. \qquad (A.11)$$

Equations (BC): 2, 3, A.10, A.11
Parameters (BC): θ_s, θ_r, α, n, K_s, λ
By substituting $n = 1/\beta$ the solution to Equation (A.1) for the BC-BW model is given as

$$S_{nc}^{pF}(x) = \begin{cases} \frac{\beta + \ln(1/\alpha)}{\ln(10)} - \frac{\beta}{\ln(10)}(\alpha 10^x)^{-\frac{1}{\beta}} - x & \alpha 10^x \geq 1 \\ 0 & \text{otherwise.} \end{cases} \qquad (A.12)$$

The unsaturated hydraulic conductivity function for the capillary part is given by:

$$K_{rc}(h) = \Phi_e(h)^{2/n+\lambda+2}. \qquad (A.13)$$

Equations (BC-BW): 4, 5, A.10, A.12, 6, A.13, A.5
Parameters (BC-BW): $\theta_{sc}, \theta_{snc}, \alpha, n, K_{sc}, K_{snc}, \lambda, \alpha_s, h_0$

A.4 | The Kosugi and Kosugi-BW models

The Kosugi (KS) (Kosugi, 1996a) effective saturation model is given as a function of pressure head by

$$\Phi_e(h) = \begin{cases} 0.5 \operatorname{erfc}\left(\frac{\ln(h/\alpha)}{\sqrt{2}n}\right) & h < 0 \\ 1 & \text{otherwise.} \end{cases} \qquad (A.14)$$

The relative hydraulic conductivity is given by

$$K_r(h) = \Phi_e(h)^\lambda \left(\frac{1}{2} \operatorname{erfc}\left[\frac{\ln(h/\alpha)}{\sqrt{2}n} + \frac{n}{\sqrt{2}}\right]\right)^2. \qquad (A.15)$$

Equations (KS): 2, 3, A.14, A.15
Parameters (KS): $\theta_s, \theta_r, \alpha, n, K_s, \lambda$

Note that in Hydrus, the symbol α instead of h_0 and n instead of σ are used, compared with the original notation in Kosugi (1996a).

Substituting $x_m = \log_{10}\alpha$ the analytical of the integral model using Equation (A.14) is

$$S_{nc}^{pF}(x) = \begin{cases} \frac{x-x_m}{2} \operatorname{erfc}\left(\frac{\ln(10)(x-x_m)}{\sqrt{2}\,n}\right) - \frac{n}{\ln(10)\sqrt{2\pi}} \\ \exp\left(-\frac{\ln^2(10)(x-x_m)^2}{2\,n^2}\right) - (x-x_m) & h < 0 \\ 0 & \text{otherwise,} \end{cases} \qquad (A.16)$$

and the hydraulic conductivity curve of the capillary pore domain is given as

$$K_{rc}(h) = S_c(h)^\lambda \left(\frac{\operatorname{erf}[\operatorname{erfc}^{-1}[2\Phi_e(h_0)] + n/\sqrt{2}] - \operatorname{erf}[\operatorname{erfc}^{-1}[2\Phi_e(h)] + n/\sqrt{2}]}{1 + \operatorname{erf}[\operatorname{erfc}^{-1}[2\Phi_e(h_0)]] + n/\sqrt{2}}\right)^2. \qquad (A.17)$$

Note that the rescaled $S_c(h)$ is used as multiplier before the bracket and Kosugi's original $\Phi_e(h)$ from Equation (A.15) in the fraction which is evaluated in two instances at $\Phi_e(h_0 = 10^{6.8})$.

Equations (KS-BW): 4, 5, A.14, A.16, 6, A.17, A.5
Parameters (KS-BW): $\theta_{sc}, \theta_{snc}, \alpha, n, K_{sc}, K_{snc}, \lambda, \alpha_s, h_0$

A.5 | The modified VGM and VGM-BW models

A more flexible model of SHPs (modVGM), proposed from Vogel and Cislerova (1988), is implemented in Hydrus. Vogel and Cislerova (1988) modified the equation of van Genuchten (1980) to add flexibility in the near saturation SHPs. The soil water retention in Equation (2) is given in an alternative form by:

$$\theta(h) = \begin{cases} \theta_\alpha + (\theta_m - \theta_\alpha)\Phi_e(h) & h < h_s \\ \theta_s & h \geq h_s, \end{cases} \qquad (A.18)$$

where $\Phi_e(h)$ is given by:

$$\Phi_e(h) = \begin{cases} \frac{1}{(1+(\alpha|h|)^n)^m} & h < h_s \\ 1.0 & h \geq h_s, \end{cases} \qquad (A.19)$$

and θ_m [L^3 L^{-3}] is a fictitious parameter slightly higher than θ_s, and θ_α [L^3 L^{-3}] is an extra parameter, with $\theta_\alpha \leq \theta_r$, that adds flexibility in the dry range of the water retention.

The relative conductivity function for the modified van Genuchten model is given by:

$$K_r(h) = \begin{cases} K_r^1(h) & h \leq h_k \\ \frac{K_k}{K_s} + \frac{(h-h_k)(K_s-K_k)}{K_s(h_s-h_k)} & h_k < h \leq h_s \\ 1.0 & h \geq h_s, \end{cases} \qquad (A.20)$$

where

$$K_r^1(h) = \frac{K_k}{K_s}\left[\frac{\Phi_e}{\Phi_{ek}}\right]^\lambda \left[\frac{F(\theta_r) - F(\theta)}{F(\theta_r) - F(\theta_k)}\right]^2, \qquad (A.21)$$

and

$$F(\theta) = \left[1 - \left(\frac{\theta - \theta_\alpha}{\theta_m - \theta_\alpha}\right)^{1/m}\right]^m \qquad (A.22)$$

$$\Phi_{ek} = \frac{\theta_k - \theta_r}{\theta_s - \theta_r}. \qquad (A.23)$$

The modified VGM model allows for a non-zero minimum capillary height h_s [L], by adjusting the value of θ_m, to a value slightly higher than θ_s. In that case, $\theta = \theta_s$ (and $K(h) = K_s$)

for $h \geq h_s$. This change has no effect on the water retention curve, but a big effect on the conductivity function, especially for fine-textured soils, with $1.0 < n \leq 1.3$ (Šimůnek, 2006). A second conductivity point (less or equal to K_s) can be provided by the user at which $K_k = K(\theta_k(h_k))$ [L T^{-1}], where the conductivity value is linearly interpolated between the two points ((h_s, K_s) and (h_k, K_k)).

A simpler version of this model is also implemented in Hydrus, where users can fix $h_s = -2$ cm, as proposed by (Vogel and Cislerova, 1988), and recommended for fine-textured soils. In that model $h_k = h_s$, $\theta_k = \theta_s$, and $K_k = K_s$.

Equations (modVGM): A.18, A.19, 3, A.20, A.21, A.22, A.23

Parameters (modVGM): $\theta_s, \theta_m, \theta_r, \theta_\alpha, \alpha, n, K_s, K_k, \theta_k, \lambda$

The Brunswick variant of the modified VGM model (modVGM-BW) is given by:

$$\theta(h) = \theta_m S_c(h) + \theta_{snc} S_{nc}(h), \qquad (A.24)$$

where θ_m is higher than θ_{sc} and $S_c(h)$ is calculated from Equation (5) where Φ_e is given by Equation (A.19).

The relative conductivity function for the capillary part in modVGM-BW is calculated by:

$$K_{rc}(h) = \begin{cases} K_{rc}^1(h) & h \leq h_k \\ \frac{K_k}{K_{sc}} + \frac{(h-h_k)(K_{sc}-K_k)}{K_{sc}(h_s-h_k)} & h_k < h \leq h_s \\ 1.0 & h \geq h_s, \end{cases} \qquad (A.25)$$

where $K_{rc}^1(h)$ is calculated by Equations (A.21–A.23), where $\theta_r = \theta_\alpha = 0$. The simpler version with $h_s = -2$ cm was also implemented. Note that for S_{nc} the function derived for the VGM model can be used directly since Φ_e is identical in the VGM-BW and modVGM-BW case.

Equations (modVGM-BW): A.24, 5, A.19, A.8, 6, A.25, A.21, A.22, A.23

Parameters (modVGM-BW): $\theta_{sc}, \theta_m, \theta_{snc}, \alpha, n, K_s, K_k, \theta_k, \lambda, a_s, h_0$